Journal of Sound and Vibration 329 (2010) 931–943

Contents lists available at ScienceDirect

Journal of Sound and Vibration

journal homepage: www.elsevier.com/locate/jsvi

On the connection between energy velocity, reverberation time and angular momentum

Domenico Stanzial [a,*], Giuliano Schiffrer [b]

[a] Italian National Research Council, Imamoter Institute, Physics Department, University of Ferrara, Room G115, v. Saragat 1, I-44100 Ferrara, Italy
[b] University of Ferrara, Physics Department, v. Saragat 1, I-44100 Ferrara, Italy

ARTICLE INFO

Article history:
Received 7 November 2008
Received in revised form
10 July 2009
Accepted 8 October 2009
Handling Editor: Y. Auregan
Available online 29 October 2009

ABSTRACT

The decay of a steady acoustic field in an enclosure is studied both theoretically and experimentally. Our main result is that the initial part of any local sound decay is driven by an exponential function of time whose rate constant is equal in modulus to the inverse of the mean energy velocity divergence. This is empirically demonstrated by experimental analysis of both 1-D and 3-D case studies, thus showing that the reverberation time is strictly connected with the sound energy velocity field and can be determined from its differential properties. A further property of the mean energy velocity is found: it is related not only with the reverberation time, but also with the angular momentum density and with the non-uniform distribution of energy.

1. Introduction

Sound energy streamlines have been firstly introduced as a new construct in acoustics, based on experimental evidence, by Waterhouse [1] in 1985. In the following years the more and more reliable experimental data showing circulation of sound energy in steady state led the same author to study energy vortices from different points of views [2,3]. About one decade later, the authors of the present paper have proposed a systematic use in acoustics of the concept of mean energy velocity [4,5] and one of them started to tantalize himself about the importance of this quantity for a refinement of reverberation time concept in acoustics [6]. At the end of the 1990s, a sharp description of intensity and vorticity streamlines in 3-D sound fields has been given in Ref. [7]. On the other hand, even earlier, a new and very effective method of measuring reverberation time was proposed by Schroeder [8], who also has designed later a device, showing that the energy of acoustic fields can rotate [9], giving rise to angular momentum. The purpose of the present paper is to outline a strict connection between energy velocity, reverberation time and angular momentum, so offering a unified physical frame where the commonly used relationships between reverberation time and absorption coefficient of the statistical model can be unambiguously checked.

After the definition of the average energy trajectories in Section 2, the analysis of sound energy density evolution along them will follow in Section 3. The purpose of Section 4 is to recall some properties of angular momentum in acoustic fields and to state its relationship with the solenoidal and irrotational parts of the energy velocity field. The experimental evidence that the theory of Section 3 is unambiguously linked to reverberation time is reported in Section 5. Section 6 is devoted to the introduction and quantitative definition of the concept of wave conductance and to analyze its relationship with energy velocity and angular momentum. Finally, the conclusion that a definition of reverberation time in acoustics

* Corresponding author.
E-mail address: domenico.stanzial@cnr.it (D. Stanzial).

0022-460X/$ - see front matter © 2009 Elsevier Ltd. All rights reserved.
doi:10.1016/j.jsv.2009.10.011

can be given in terms of the divergence of the energy velocity and that the measure of this quantity could be standardized thanks to hyper-intensimetric measurements and fine calibrations of sound intensity probes, is drawn in the last section.

2. The average energy trajectories

We start from the acoustic energy conservation law, written in the form

$$\frac{\partial w}{\partial t} + \boldsymbol{\nabla} \cdot \boldsymbol{j} = 0, \tag{1}$$

where the energy density w and the energy flux density $\boldsymbol{j}$ (sound intensity) are defined in terms of the acoustic field variables, the pressure p and the velocity $\boldsymbol{v}$, as

$$w(\boldsymbol{x},t) = \frac{1}{2}\rho_0 \left[\left(\frac{p(\boldsymbol{x},t)}{\rho_0 c} \right)^2 + \boldsymbol{v}(\boldsymbol{x},t)^2 \right], \quad \boldsymbol{j}(\boldsymbol{x},t) = p(\boldsymbol{x},t)\boldsymbol{v}(\boldsymbol{x},t). \tag{2}$$

Here, $\boldsymbol{x}$ and t are space and time coordinates, c the speed of sound and ρ_0 the equilibrium density of the gas medium. Since the instantaneous quantities $\boldsymbol{j}(\boldsymbol{x},t)$ and $w(\boldsymbol{x},t)$ are too rapidly varying functions of time, it is convenient to perform on them some kind of average. Although all the considerations of this section hold for all kinds of average, we shall be concerned later with the stationary average, defined by

$$\langle u \rangle(\boldsymbol{x}) = \lim_{T\to\infty} \frac{1}{2T} \int_{-T}^{+T} u(\boldsymbol{x},t)\,\mathrm{d}t$$

or

$$\langle u \rangle(\boldsymbol{x}) = \lim_{T\to\infty} \frac{1}{T} \int_{-T}^{0} u(\boldsymbol{x},t)\,\mathrm{d}t$$

for any function u. In the present paper the only properties which shall be required to any averaging procedure $\langle \cdot \rangle$ are

$$\left\langle \frac{\partial u}{\partial t} \right\rangle = \frac{\partial \langle u \rangle}{\partial t}, \quad \langle \boldsymbol{\nabla} \cdot \boldsymbol{u} \rangle = \boldsymbol{\nabla} \cdot \langle \boldsymbol{u} \rangle, \quad \langle \boldsymbol{\nabla} \wedge \boldsymbol{u} \rangle = \boldsymbol{\nabla} \wedge \langle \boldsymbol{u} \rangle,$$

where $u(\boldsymbol{x},t)$ and $\boldsymbol{u}(\boldsymbol{x},t)$ are any scalar, respectively, vector field. All usual averaging procedures, such as Schroeder's back-integration, stationary and space average share these properties. Thus, by averaging (1), we get

$$\frac{\partial W}{\partial t} + \boldsymbol{\nabla} \cdot \boldsymbol{J} = 0, \tag{3}$$

where $W \overset{\text{def}}{=} \langle w \rangle$, $\boldsymbol{J} \overset{\text{def}}{=} \langle \boldsymbol{j} \rangle$. Of course, in the case of a stationary averages the further property

$$\frac{\partial \langle u \rangle}{\partial t} = 0$$

holds for any generic field u and thus Eq. (3) reduces to the well known property $\boldsymbol{\nabla} \cdot \boldsymbol{J} = 0$ of the so called active sound intensity $\boldsymbol{J}$.

As explained in [4], the instantaneous quantities $\boldsymbol{j}(\boldsymbol{x},t)$ and $w(\boldsymbol{x},t)$ can be combined to obtain a new vector field $\boldsymbol{u} = \boldsymbol{j}/w$, which is interpreted as energy velocity. This instantaneous vector field can be averaged in turn to obtain the average quantity $\langle \boldsymbol{j}/w \rangle$. However, we shall not adopt this definition of mean energy velocity, because its direction is, in general, different than the direction of the mean momentum of the acoustic field, which is

$$\langle \boldsymbol{q} \rangle = \frac{\langle \boldsymbol{j} \rangle}{c^2} = \boldsymbol{Q}. \tag{4}$$

Therefore, the adopted definition will be the following.

Definition 1. The average energy velocity $\boldsymbol{U}$ is defined as the ratio $\boldsymbol{J}/W$:

$$\boldsymbol{U} = \frac{\langle \boldsymbol{j} \rangle}{\langle w \rangle} = \frac{\boldsymbol{J}}{W} = \frac{c^2 \boldsymbol{Q}}{W}. \tag{5}$$

We are now in the position for putting forward the analogy between a fluid motion and sound energy motion. This is done by assimilating the fluid mass density to the average sound energy density $\rho_{\text{fluid}} \leftrightarrow \langle w \rangle_{\text{energy}}$ and the fluid velocity to the average sound energy velocity $\boldsymbol{v}_{\text{fluid}} \leftrightarrow \boldsymbol{U}_{\text{energy}}$, so as to define in strict analogy to fluid dynamics the concept of energy trajectories. In fact, the *energy trajectory* initially ($t = 0$) starting at point $\boldsymbol{x}_0$,

$$\boldsymbol{x} = \boldsymbol{s}(\boldsymbol{x}_0, t)$$

is defined by the differential equation with initial condition

$$\frac{\mathrm{d}\boldsymbol{s}(\boldsymbol{x}_0,t)}{\mathrm{d}t} = \boldsymbol{U}(\boldsymbol{s}(\boldsymbol{x}_0,t),t); \quad \boldsymbol{s}(\boldsymbol{x}_0,0) = \boldsymbol{x}_0. \tag{6}$$

It is seen from this equation that every point $\boldsymbol{x}_0$ in the domain occupied by the acoustic field can be thought as a starting point of a trajectory, representing the average motion of energy in the field.

The stationary average will be preferred here to other kinds of average, because it has a remarkable property: the energy trajectories coincide with energy streamlines [11].

3. Energy density evolution along trajectories and reverberation time

We first prove a theorem, stating how stationary energy density in an enclosure evolves in time, following energy trajectories. This theorem could be exploited, as we shall see in Section 5, for a new procedure of defining and measuring the reverberation time and exhibits, in our opinion, a better physical foundation than the current ones. In fact, the proof of this theorem is a direct consequence of one of the pillars of linear acoustics, the continuity equation (3) that—once reformulated in terms of the energy velocity as defined in (5)—can be clearly interpreted as the transport equation of sound energy along steady streamlines, coinciding with the trajectories of sound energy particles (body energy). The practical important consequence of this approach is that it is always possible to foresee the initial rate of any transient sound energy decay caused by the breakdown of the steady state condition by means of a local measurement of stationary energetic properties of the sound field. Let $t=0$ be the arbitrary time when the average energy density (energy particle) passes through the point $\boldsymbol{s}(\boldsymbol{x}_0,0)=\boldsymbol{x}_0$ of its (stationary) trajectory and suppose that in the same instant the energy decay begins at $\boldsymbol{x}_0$ as a consequence of the switching off of the sources. Then the following theorem holds.

Theorem 2. *The time evolution of the average energy density W in a neighborhood of $t=0$ along the energy trajectory starting at any point $\boldsymbol{x}_0$ is given by an exponential law*:

$$W(\boldsymbol{s}(\boldsymbol{x}_0,t),t)=W_0\exp\frac{-t}{\tau_0}, \tag{7}$$

where

$$W_0=W(\boldsymbol{x}_0,0),\quad \tau_0=\frac{1}{\boldsymbol{\nabla}\cdot\boldsymbol{U}(\boldsymbol{x},0)|_{\boldsymbol{x}_0}}. \tag{8}$$

Proof. We can eliminate $\boldsymbol{J}$ from Eq. (3) by introducing there the velocity $\boldsymbol{U}$:

$$\frac{\partial W}{\partial t}+\boldsymbol{\nabla}\cdot(W\boldsymbol{U})=0.$$

By expanding the divergence and moving to the right hand side the term containing $\boldsymbol{\nabla}\cdot\boldsymbol{U}$, this becomes

$$\frac{\partial W}{\partial t}+\boldsymbol{U}\cdot\boldsymbol{\nabla}W=-W\boldsymbol{\nabla}\cdot\boldsymbol{U}.$$

After division by W, this equation can be rewritten as

$$\frac{\mathrm{d}\ln W}{\mathrm{d}t}=-\boldsymbol{\nabla}\cdot\boldsymbol{U}, \tag{9}$$

where

$$\frac{\mathrm{d}}{\mathrm{d}t}\overset{\mathrm{def}}{=}\frac{\partial}{\partial t}+\boldsymbol{U}\cdot\boldsymbol{\nabla}$$

is the Lagrangian differentiation operator along the energy trajectory defined by (6). Eq. (9) can be integrated in an infinitesimal neighborhood of $t=0$. To this purpose, we introduce the function of time

$$D_0(t)\overset{\mathrm{def}}{=}\boldsymbol{\nabla}\cdot\boldsymbol{U}(\boldsymbol{x},t)|_{\boldsymbol{x}=\boldsymbol{s}(\boldsymbol{x}_0,t)},$$

representing the divergence of $\boldsymbol{U}$ along the trajectory. Assuming $D_0(t)$ to be infinitely differentiable, this function can be expanded into a Taylor series around $t=0$, so that

$$D_0(t)=D_0(0)+D_0'(0)t+\cdots,$$

with $D_0(0)=\boldsymbol{\nabla}\cdot\boldsymbol{U}(\boldsymbol{x}_0,0)$. Introducing the expansion of D_0 into Eq. (9), we get

$$\frac{\mathrm{d}\ln W}{\mathrm{d}t}=-[D_0(0)+D_0'(0)t+\cdots],$$

whose solution is

$$W(\boldsymbol{s}(\boldsymbol{x}_0,t),t)=W_0\exp\{-[D_0(0)t+\tfrac{1}{2}D_0'(0)t^2+\cdots]\}. \tag{10}$$

This can be written

$$W(\boldsymbol{s}(\boldsymbol{x}_0,t),t)=W_0\exp[-D_0(0)t]V(t),$$

where $V(t) = 1 + \mathcal{O}(t^2)$, as $t \to 0$. Therefore, in this limit we have

$$W(\boldsymbol{s}(\boldsymbol{x}_0, t), t) = W_0 \exp[-D_0(0)t]. \qquad \square \tag{11}$$

The theorem cannot say more on the size of the neighborhood of $t = 0$, where the Eq. (11) holds. It simply states that whenever the energy particle density undergoes an instantaneous variation during its stationary motion, the first-order approximation to this variation is given by an exponential function of time having a rate constant equal to the divergence of the energy particle velocity. That is all.

This property, which could seem to be of limited interest in stationary fields, becomes instead a very useful practical tool when used for estimating the initial slope of any sound decay starting in $\boldsymbol{x}_0$ at the instant $t = 0$. This fact will be experimentally tested in Section 5 for several carefully chosen acoustic situations. In other words, the importance of the above stated theorem is that the first-order exponential approximation to the steady-state energy evolution just before the decay, remains unchanged for a while even during the decay itself, so allowing to use the same exponential approximation also for guessing the initial slope of the decay. The generality of this statement is truly impressive, keeping in mind that all practical situations of interest in room acoustics are characterized by exponential-like decays [12–14], and consequently, in these cases, the decay rate constant determined from τ_0 is indeed a good estimate of the most significant part of the decay. The worst cases are met, instead, in acoustical situations when energy decays in bizarre ways, appearing to be very far from exponential-like decays. These unpleasant situations are analyzed in detail in Section 5, finding that even in these cases the above general statement holds true.

We propose, therefore, a precise definition of *initial decay time*: it is the time t, belonging to any interval $0 < t < \tau_1$, when the sound energy density decay displays an exponential-like time evolution similar to Eq. (11), but on a statistical and not instantaneous basis.

4. Does the angular momentum of acoustic fields influence the reverberation time?

All acoustic fields contain, besides energy, linear momentum, as well as angular momentum. We have already developed a theoretical treatment of this subject in [10] and earlier work was done by other authors [1–3,9]. Nevertheless, we think it would be convenient for the reader to have here a short account of the main concepts, both for better analyzing the connection between reverberation time and angular momentum and in view of the developments of Section 6.

As said above, the density of linear momentum is given by $\boldsymbol{q} = \boldsymbol{j}/c^2$ and its average value by $\boldsymbol{Q} = \boldsymbol{J}/c^2$, Eq. (4). The conservation law in free space is [10]

$$\frac{\partial \boldsymbol{q}}{\partial t} + \boldsymbol{\nabla} \cdot \mathscr{T} = \boldsymbol{0},$$

where $\mathscr{T}$ is the acoustic stress tensor, representing the momentum flux density, whose Cartesian components are

$$t_{ij} = \rho_0 v_i v_j + \frac{1}{2}\left(\frac{p^2}{\rho_0 c^2} - \rho_0 \boldsymbol{v}^2\right)\delta_{ij}.$$

The same equation holds also for the averages

$$\frac{\partial \boldsymbol{Q}}{\partial t} + \boldsymbol{\nabla} \cdot \mathfrak{T} = \boldsymbol{0},$$

where $\mathfrak{T} = \langle \mathscr{T} \rangle$.

The linear momentum density $\boldsymbol{q}$ gives rise to the angular momentum density $\boldsymbol{l} = \boldsymbol{x}_0 \wedge \boldsymbol{q}$ with respect to a fixed point $\boldsymbol{x}_0$. Averaging this expression, one obtains

$$\langle \boldsymbol{l} \rangle = \boldsymbol{L} = \boldsymbol{x}_0 \wedge \boldsymbol{Q}, \tag{12}$$

with the conservation law:

$$\boldsymbol{x}_0 \wedge \left(\frac{\partial \boldsymbol{Q}}{\partial t} + \boldsymbol{\nabla} \cdot \mathfrak{T}\right) = \boldsymbol{0}.$$

Typical examples of angular momentum of acoustic fields have been treated in Refs. [2,3,9]. Schroeder [9] realized an experimental device for the direct detection of rotational acoustic energy; it is based on two loudspeakers assembled orthogonally to each other, exciting the axial modes in a box of base $l \times l$ and height h. He fed the loudspeakers by two sinusoidal signals having the same circular frequency ω and a phase difference φ, showing that rotating sound energy sets a small absorbing wheel into rotation around the $z-$axis. If the walls are considered to be perfectly reflective, it is easy to find from Eq. (12) that the average angular momentum density with respect to the fixed point $\boldsymbol{x}_0 = x_0\boldsymbol{e}_x + y_0\boldsymbol{e}_y + z_0\boldsymbol{e}_z$ is

$$\begin{aligned} \boldsymbol{L}(x,y,z) &= \frac{1}{c^2}[x_0 J_y(x,y,z) - y_0 J_x(x,y,z)]\boldsymbol{e}_z \\ &= \frac{1}{2}\rho_0 c (kA)^2 \sin(\varphi)[x_0 \sin(kx)\cos(ky) + y_0 \cos(kx)\sin(ky)]\boldsymbol{e}_z, \quad -\frac{l}{2} \le x \le \frac{l}{2}, \quad -\frac{l}{2} \le y \le \frac{l}{2}, \quad 0 \le z \le h, \end{aligned} \tag{13}$$

where only the two lowest modes have been included and the boundary conditions imply $k=\pi/l=\omega/c$. The average intensity is

$$\boldsymbol{J}(x,y,z)=\tfrac{1}{2}\rho_0 c(\omega A)^2[\cos(kx)\sin(ky)\boldsymbol{e}_x-\sin(kx)\cos(ky)\boldsymbol{e}_y]\sin\varphi,$$

where A is the amplitude of both modes. The average energy velocity of the field is

$$\boldsymbol{U}(x,y,z)=\frac{c[\cos(kx)\sin(ky)\boldsymbol{e}_x-\sin(kx)\cos(ky)\boldsymbol{e}_y]\sin\varphi}{1+\frac{1}{2}\sin(kx)\sin(ky)\cos\varphi}.$$

The stationary average angular velocity $\boldsymbol{\Omega}$ of acoustic energy can be expressed in terms of the intensity $\boldsymbol{J}$ and energy density W as

$$\boldsymbol{\Omega}(\boldsymbol{x})=\frac{1}{2}\boldsymbol{\nabla}\wedge\boldsymbol{U}(\boldsymbol{x})=\frac{1}{2}\boldsymbol{\nabla}\wedge\frac{\boldsymbol{J}(\boldsymbol{x})}{W(\boldsymbol{x})}=\frac{\boldsymbol{\nabla}\wedge\boldsymbol{J}+\boldsymbol{J}\wedge\boldsymbol{\nabla}\ln W}{2W}. \tag{14}$$

Writing this formula as

$$\boldsymbol{\Omega}=\boldsymbol{\Omega}_1+\boldsymbol{\Omega}_2,$$

with

$$\boldsymbol{\Omega}_1\stackrel{\text{def}}{=}\frac{\boldsymbol{\nabla}\wedge\boldsymbol{J}}{2W},\quad \boldsymbol{\Omega}_2\stackrel{\text{def}}{=}\frac{\boldsymbol{J}\wedge\boldsymbol{\nabla}\ln W}{2W}, \tag{15}$$

it is seen that the expression for $\boldsymbol{\Omega}_1$ is that of the statistical model of diffuse sound field, which assumes $\boldsymbol{\nabla}W=0$, i.e. a uniform energy distribution; according to the result quoted by Waterhouse [3], stating that $\boldsymbol{\nabla}\wedge\boldsymbol{J}=\omega^2\boldsymbol{L}$, this term vanishes with the angular momentum density $\boldsymbol{L}$:

$$\boldsymbol{\Omega}_1=\frac{\omega^2\boldsymbol{L}}{2W}.$$

The term $\boldsymbol{\Omega}_2$ is due to non-uniformity of energy distribution.

We have just seen in Section 3 how the divergence of the energy velocity is strictly connected with decay time of the field in an enclosure. Since any vector field can be decomposed into the sum of an irrotational and a solenoidal one and the field itself can be reconstructed from its divergence and its curl, it is natural to look for an expression relating the energy velocity field to the reverberation time and the angular momentum of the field.

Thus, we can write

$$\boldsymbol{U}=\boldsymbol{U}_{\text{irr}}+\boldsymbol{U}_{\text{sol}},\quad \boldsymbol{\nabla}\wedge\boldsymbol{U}_{\text{irr}}\stackrel{\text{def}}{=}\boldsymbol{0},\quad \boldsymbol{\nabla}\cdot\boldsymbol{U}_{\text{sol}}\stackrel{\text{def}}{=}0. \tag{16}$$

The reverberation time depends only on $\boldsymbol{U}_{\text{irr}}$, since

$$\boldsymbol{\nabla}\cdot\boldsymbol{U}=\boldsymbol{\nabla}\cdot(\boldsymbol{U}_{\text{irr}}+\boldsymbol{U}_{\text{sol}})=\boldsymbol{\nabla}\cdot\boldsymbol{U}_{\text{irr}},$$

while the rotation of energy depends only on $\boldsymbol{U}_{\text{sol}}$, because

$$\boldsymbol{\nabla}\wedge\boldsymbol{U}=\boldsymbol{\nabla}\wedge(\boldsymbol{U}_{\text{irr}}+\boldsymbol{U}_{\text{sol}})=\boldsymbol{\nabla}\wedge\boldsymbol{U}_{\text{sol}}.$$

It is then clear that the irrotational component $\boldsymbol{U}_{\text{irr}}$ of the energy velocity $\boldsymbol{U}$ is the only component of $\boldsymbol{U}$ related to the energy decay in any enclosure.

5. Experimental estimate of reverberation time from the exponential initial decay

Let us now give the experimental evidence that any statistical decay of sound from its steady state can be well guessed by an exponential function of time similar to (7), $\exp(-kt)$, in general with $k=|1/\tau_0|$. In fact, according to the energy conservation law, a complete decay of sound from any steady state is only permitted if $k>0$. More explicitly, the energy density at a given point according to Schroeder's picture cannot increase in time. On the other hand, the stationary energy density W along a trajectory does not share this property. As a consequence, the quantity $\boldsymbol{\nabla}\cdot\boldsymbol{U}$ is not expected to be necessarily positive, although it was in all cases we have measured. For this reason, we have introduced the definition $k\stackrel{\text{def}}{=}|\boldsymbol{\nabla}\cdot\boldsymbol{U}(\boldsymbol{x},0)|$ for the decay constant.

We shall call k the local rate constant of the exponential initial decay of sound and abandon, in this section, the stationary view of energy motion along trajectories in favor of a transient picture, which more closely describes the sound decay.

As known, the relationship between the stationary and transient states of sound is numerically synthesized in the Schroeder's energy curve derivable from back-integration of the room impulse response [8]. The systematic application of this almost 50 years old finding, to both pressure and air particle velocity impulse responses measured in any room, allows nowadays to develop a robust and precise experimental method for defining and measuring the reverberation time using intensimetric techniques. In fact, as it will be shown in the following, the only thing we have to do, is to carry out a precision measurement of k, i.e. the absolute value of the divergence of the stationary energy velocity field at the same point where the reverberation time has to be estimated.

In order to measure k from the divergence of the energy velocity $D_0(0)$ appearing in Eq. (11), the following expression has been used:

$$k := |D_0(0)| = |\nabla \cdot \boldsymbol{U}(\boldsymbol{x},0)|_{\boldsymbol{x}=\boldsymbol{x}_0}| = \left|\nabla \cdot \frac{\boldsymbol{J}(\boldsymbol{x})}{W(\boldsymbol{x})}\bigg|_{\boldsymbol{x}=\boldsymbol{x}_0}\right| = \left|-\frac{1}{W^2(\boldsymbol{x}_0)}\sum_{i=1}^{3} J_i \frac{\partial W}{\partial x_i}\bigg|_{\boldsymbol{x}=\boldsymbol{x}_0}\right|, \tag{17}$$

where we have taken into account that $\nabla \cdot \boldsymbol{J} = 0$. The evaluation of k from experimental data requires at least two simultaneous measurements of the energy density along each spatial dimension in the neighborhood of the measurement point. This has been done by means of a well calibrated pair of pressure–velocity sound intensity probes (i.e. a special array of $p-v$ probes, which we call hyper-intensimetric probe: see Figs. 1 and 2). In fact, previously to the here reported measurement campaign, each axial sound intensity probe used for experiments has undergone a fine calibration process [15]. Our calibration process is similar in principle to the ones reported in literature [16] but using as a reference field of known impedance, the sound field generated inside a "semi-infinite" acoustical waveguide having a high frequency cutoff of about 10 kHz and a length of 84 m. As well documented in [17], the field within such a waveguide is characterized by a constant pure resistive load equal to the characteristic impedance of air. This forces the sound to propagate in the form of a plane progressive wave, with no reflected wave, whose amplitude—due to thermoviscous losses occurring in the boundary layer very near to the internal cylindrical surface—attenuates, of course, with increasing distance from the sound source, without changing the wave impedance.

The robustness of the resulting experimental methodology for measuring k has been checked firstly in the worst conditions like those encountered in 1-D environments, where sound energy abruptly drops during the decay. Once this

Fig. 1. The special mount with the pair of match size axial sound intensity probes: during the measurement the two probes are aligned along any coordinate axis. Note the anemometric bridge of the two velocity sensors.

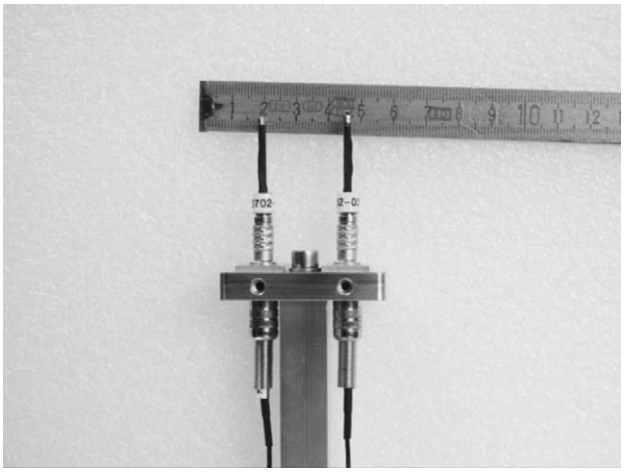

Fig. 2. The pair of match size axial sound intensity probes assembled in the hyper-probe are mounted 2.5 cm apart from each other.

shock test was successfully passed, the same methodology has been applied to a more traditional 3-D environment (the authors' 104 m^3 laboratory) where, according to the common practice of room acoustics measurements, it has been found that the exponential curve obtained from k, nicely fits in the Schroeder's energy curve.

Here follows the report of obtained results.

5.1. 1-D case study

The test environment for 1-D experiments was set up with a 4 m long tube having a square section of $0.28 \times 0.28\ m^2$ and equipped with a loudspeaker source mounted at one end. The other end of the tube has been furnished with boundaries of different sound absorbing power: a foam rubber panel, a wooden panel or, more simply, by leaving open its termination (open end).

In order to excite only longitudinal modes of the air inside the tube, the loudspeaker source was fed by a 50–600 Hz band swept-sine signal. A finely calibrated hyper-intensity probe was located along the axis of the tube at 1.5 m from the loudspeaker. Two pair of pressure and velocity signals for a total of four signals, were captured by means of this special probe and then processed with proper deconvolution MatLab™ routines in order to calculate the respective pairs of pressure and velocity impulse responses. As shown in Fig. 2, the distance between the two match size Microflown™ axial intensity probes assembled in the hyper-probe mount is 2.5 cm.

Table 1
Steady-state energy level, divergence of energy velocity and $k-$reverberation time for all case studies.

	1-D Rubber	1-D Open	1-D Wood	3-D Small room
L_{SSE} (dB)	112.9	114.9	115.6	101.3
k	129.40	35.33	36.64	23.96
T_{k60} (s)	0.11	0.39	0.38	0.58

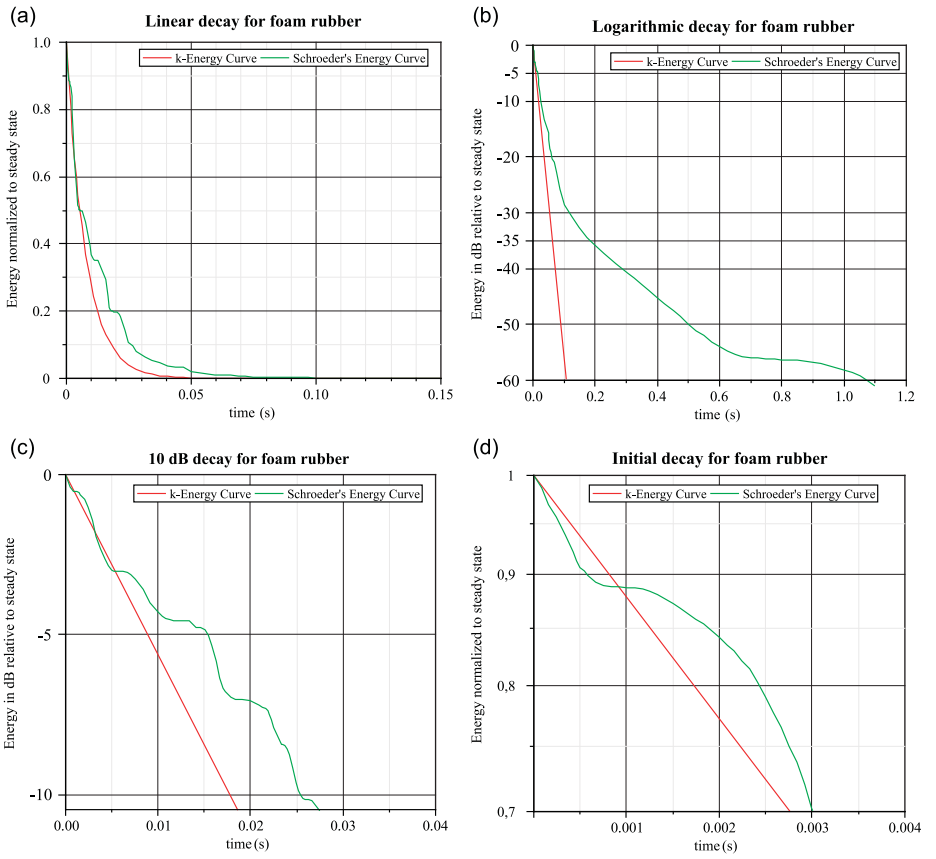

Fig. 3. 1-D case study for foam rubber.

The raw pressure and air velocity impulse responses measured in the above described 1-D acoustic system have been finally filtered by using calibration data obtained with the above described waveguide methodology. It has been verified that the calibration process described in [15] allows to determine the average value of the sound energy density just before its decay with a maximum deviation of −0.53 dB relative to the first sample value of the Schroeder's energy curve for all 1-D case studies here reported. The corrected values have thus been used as the steady-state energy values, to which, both the Schroeder's energy curves and the exponential curves obtained from k for each case study have been normalized. The energy levels of these steady-state values expressed in dB relative to $10^{-12}\,\mathrm{J/m^3}$ are reported in Table 1 as L_{SSE}.

In the 1-D case considered here, the expression (17) has been approximated by the finite-difference ratio:

$$k \approx \frac{1}{W(x_0)^2} \times \left| \frac{J_1(x_0)[W(x_0+\Delta x) - W(x_0-\Delta x)]}{2\Delta x} \right|, \tag{18}$$

where $\Delta x = 1.25$ cm. The numerical post-processing of the two sets of pressure and velocity impulse responses calculated from signals coming from the calibrated sound intensity hyper-probe, has been implemented using a MAPLE™ worksheet. The algorithm calculates the steady-state quantities appearing on the right side of Eq. (18) using the Schroeder's back integration averaging process and determines the value of the rate constant k, so allowing the direct comparison of the energy exponential decay foreseen by k with the plot of the experimental decay curve (Schroeder's energy curve) both normalized to the steady state value of the energy density assumed as the starting value of the decay.

Obtained results are reported in Figs. 3–5 respectively for the foam rubber, open end, and wooden panel case. In each figure the (a) labeled plots show the comparison between exponential decays calculated using the rate constant k of Eq. (18) and the corresponding Schroeder's energy curve. In the (b) labeled plots of each figure, the logarithmic decays are shown, explicitly marking the −5 and −35 dB line levels in order to allow the easy comparison with the ISO 3382 standard. In the (c) labeled plots of each case study, the −10 dB decay has been zoomed-in so to render a sharper picture of the excellent experimental fitting of the exponential decay foreseen by k with the Schroeder's one. Finally, in the (d) labeled plots, the very beginning of any decay has been extra zoomed-in so making absolutely clear that there is no general relation between the slope of the exponential decay and the initial slope of the Schroeder's energy curve. Simply the rate constant k, calculated in the stationary state when the sound source is in a dynamic equilibrium with the sound field, optimally

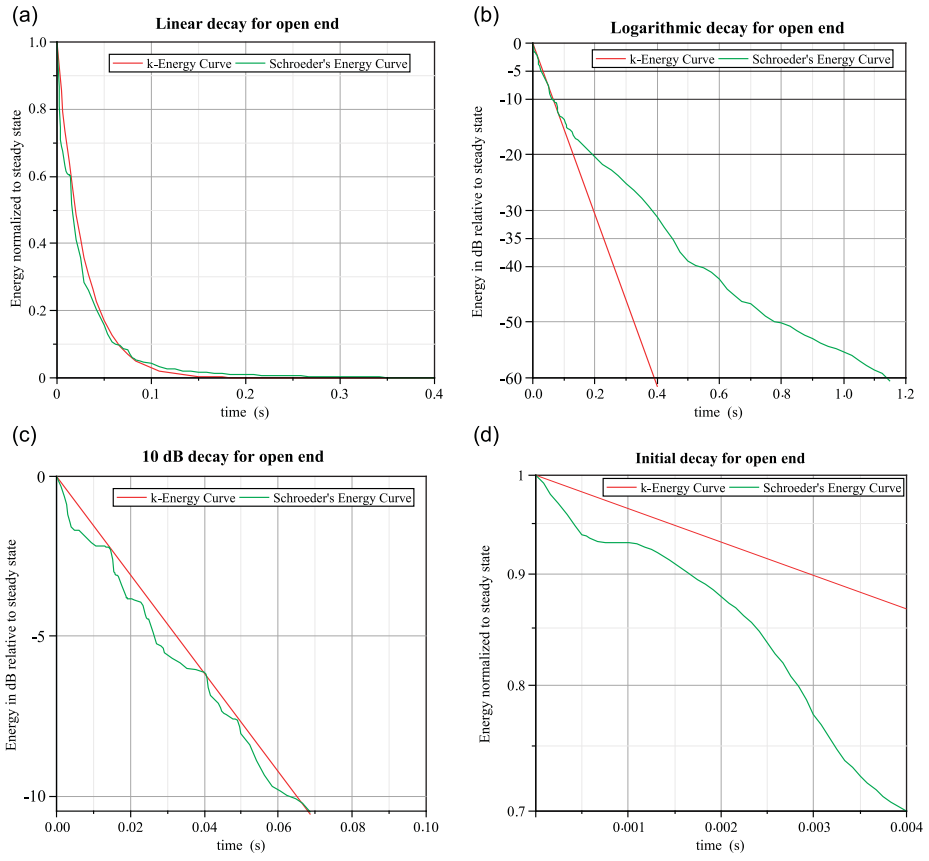

Fig. 4. 1-D case study for open end.

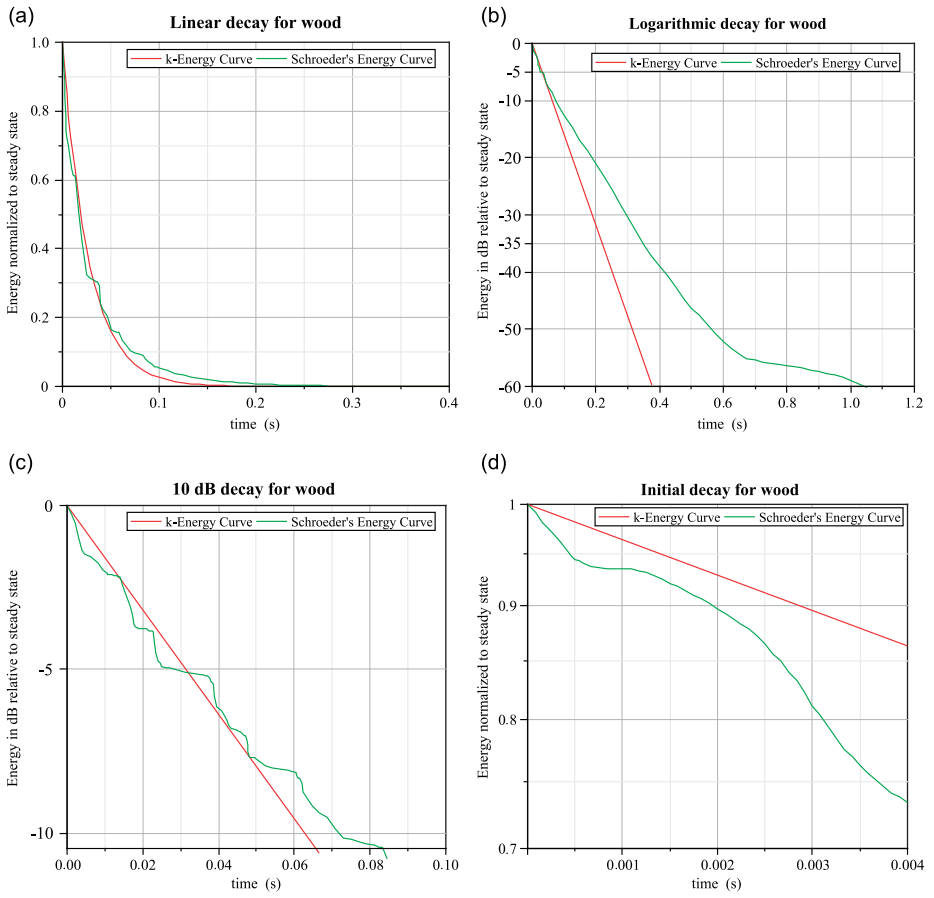

Fig. 5. 1-D case study for wood.

addresses the statistical decay starting at the measurement point when the effect of the sound source switching-off, abruptly appears. This is of course a catastrophic event during which the coincidence of the energy particle trajectories with power streamlines gets lost. Anyway, it is evident from the (c) labeled plots that this is not an instantaneous process since a time τ_1 exists, such that $0<t<\tau_1$ when the statistical local decay is well driven by the exponential curve. In the three reported case studies τ_1 is always empirically found to be at least 5×10^{-3} s.

5.2. 3-D case study

As said above, the chosen test environment for 3-D experiments was the authors' acoustics laboratory collocated in the 104 m^3 room G115 of the Physics Department. The measurement set-up has been arranged there supplying the loudspeaker source with a swept-sine signal in the 50–5000 Hz band. Given the 3-D nature of the generated sound field, the hyper-intensimetric probe of Fig. 2 was mounted on a special support allowing to align the hyper-probe axis along the $x,y,z-$axes of a Cartesian coordinate system (see Fig. 6).

The room is a parallelepiped with a stoneware tile floor ($5.92\times5.48\ m^2$), a plaster panel ceiling and concrete brick walls. It is mainly furnished with glass, hard plastic and metal. The measurement point has been located at about 2 m from the source in front of a large windows ($3.6\times1.5\ m^2$) closed with double-glazed panels of glass.

When measurements in 3-D sound fields have to be carried out, the formula for computing the value of k has to take into account the calculation of the three components of the gradient of energy density so generalizing according to Eq. (17) the finite difference approximation given by (18). Also the calibration process has to be extended to the three pairs of raw $p-v$ impulse responses sampled along the x,y,z-axes resulting in a total of 12 measured and calibrated impulse responses. Given the time invariant nature of the acoustic system the measurement process has been accomplished in three subsequent stages having care of keeping unchanged the boundary conditions.

Fig. 7 shows the obtained results ordered and labeled as for 1-D case studies. The interesting thing to remark here looking at the (c) labeled plot is the impressive fit that the k-curve operates over the Schroeder's one in the $[0,\tau_1\approx0.04\,s]$ interval. This is well confirmed here even by the extra-zoomed plot reported in the (d) frame where the Schroeder's curve bounces sharply a least three times against the k-curve in less than two-hundredth of a second.

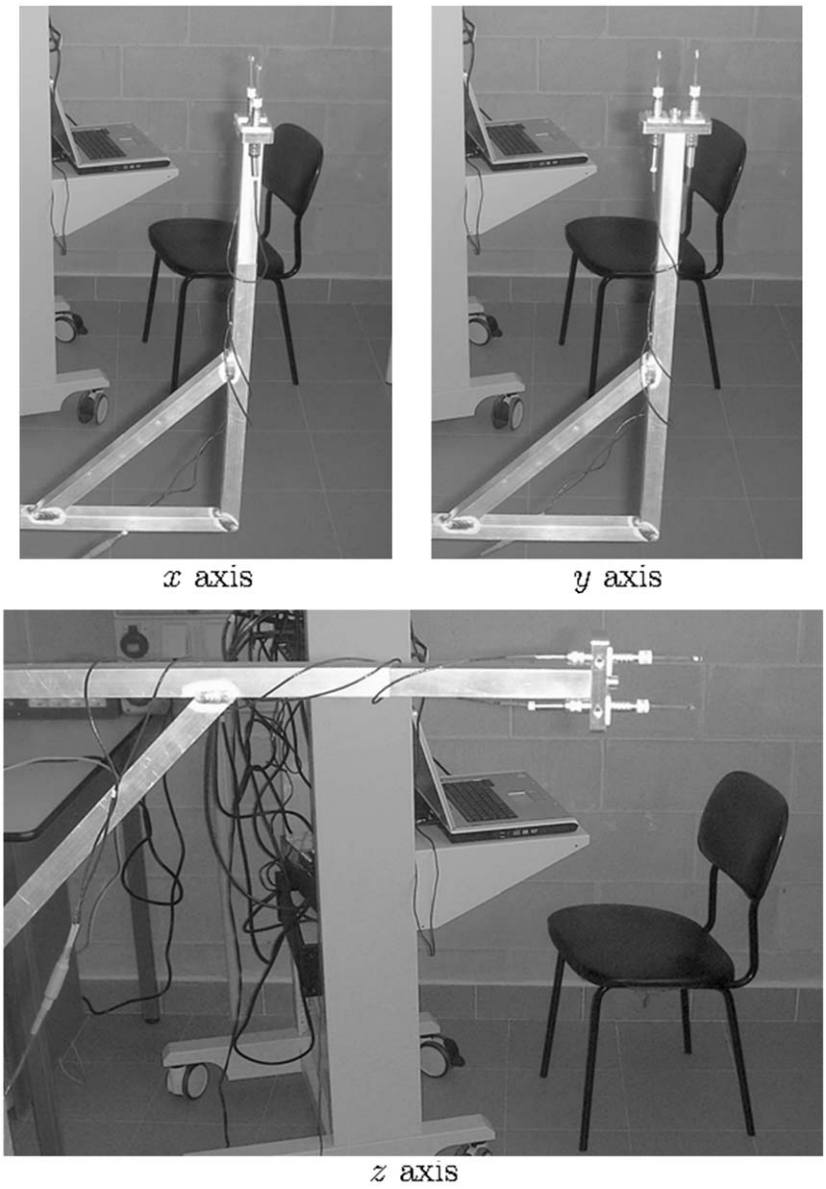

Fig. 6. The 3-D Cartesian coordinate system in room G115.

Finally the deviation of −0.65 dB relative to the first sampled value of the Schroeder's energy curve got for this case study, demonstrated the robustness of the *k*-algorithm even in 3-D environments.

We close this section summarizing in Table 1 results obtained for L_{SSE}, k and the associated k-reverberation time T_{k60} extrapolated from the exponential initial decay for all 1-D and 3-D cases studied here.

6. The concept of wave conductance and its connection to reverberation time and rotational energy

Considering the energy propagation in sound fields, the usual definition of impedance in acoustics can be interpreted in the following physical terms: it is the ratio of the power $\mathrm{d}\Pi$ per unit area, crossing normally the surface element with normal $\hat{\boldsymbol{n}}$ and area $\mathrm{d}\Sigma$, to the *energy per unit mass*, which is usually taken to be simply twice the average kinetic energy, i.e. $\boldsymbol{v}^2$:

$$z(\boldsymbol{x}, t, \hat{\boldsymbol{n}}) = \frac{1}{\boldsymbol{v}^2}\frac{\mathrm{d}\Pi}{\mathrm{d}\Sigma} = \frac{\hat{\boldsymbol{n}} \cdot \boldsymbol{j}}{\boldsymbol{v}^2}.$$

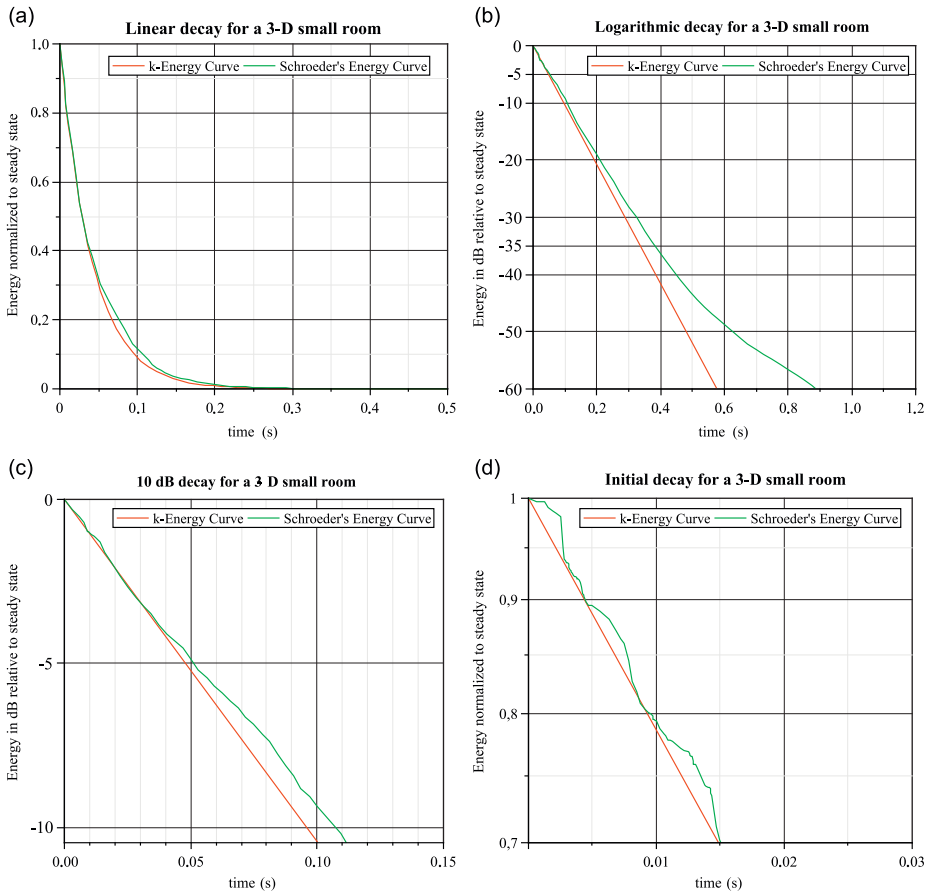

Fig. 7. 3-D small room case study.

In fact, in the case of a plane, purely progressive wave, taking as $\hat{\boldsymbol{n}}$ the direction of $\boldsymbol{J}$, this definition leads to the familiar result

$$z(\boldsymbol{x}, t, \hat{\boldsymbol{n}}) = \frac{|p(\boldsymbol{x}, t)|}{|\boldsymbol{v}(\boldsymbol{x}, t)|} = \rho_0 c = z_0.$$

Needless to say, for a different kind of wave, the impedance is neither given by the ratio $|p|/|\boldsymbol{v}|$, nor by the constant z_0; it depends on the position $\boldsymbol{x}$ and can be singular, as happens, for instance, to a stationary wave in the nodes of $\boldsymbol{v}$.

The singularities can be avoided if we take in place of $\boldsymbol{v}^2$ the exact value of the energy per unit mass, w_{m}, (mass-specific energy), including also the part proportional to p^2:

$$w_{\mathrm{m}} = \frac{w}{\rho_0} = \frac{1}{2}\left[v^2 + \left(\frac{p}{z_0}\right)^2\right].$$

Thus, it is convenient to define a new quantity, which we propose to call *wave conductance S*, as the ratio of the mean power $\mathrm{d}\Pi$ per unit area, crossing the surface element of normal $\hat{\boldsymbol{n}}$ and area $\mathrm{d}\Sigma$ to the mass-specific average energy of the field itself. Thus, we write

$$S(\boldsymbol{x}, \hat{\boldsymbol{n}}) = \frac{\rho_0}{\langle w \rangle}\frac{\mathrm{d}\Pi}{\mathrm{d}\Sigma} = \frac{2}{\left\langle \boldsymbol{v}^2 + \left(\frac{p}{z_0}\right)^2 \right\rangle}\frac{\mathrm{d}\Pi}{\mathrm{d}\Sigma} = \frac{2\hat{\boldsymbol{n}} \cdot \langle \boldsymbol{j} \rangle}{\left\langle \boldsymbol{v}^2 + \left(\frac{p}{z_0}\right)^2 \right\rangle}.$$

Another advantage of introducing S is that this quantity can be written quite simply for all kind of fields, using the parameter η, introduced in Ref. [5]:

$$\eta \overset{\mathrm{def}}{=} \frac{|\langle \boldsymbol{j} \rangle|}{c\langle w \rangle}. \tag{19}$$

The most obvious physical meaning of η is that of energy velocity in units of c. It follows that the wave conductance in the direction of $\langle \boldsymbol{j} \rangle$, $\hat{\boldsymbol{n}} = \langle \boldsymbol{j} \rangle / |\langle \boldsymbol{j} \rangle|$, is proportional to η, the proportionality constant being just the impedance z_0 of a purely

progressive plane wave:

$$S(\boldsymbol{x},\hat{\boldsymbol{n}}) = z_0\eta(\boldsymbol{x}) \leq z_0.$$

According to the above construction, it is seen that the physical meaning of η is that of a fraction of the total energy carried by a progressive-like wave, moving ahead with speed c in the direction of $\langle \boldsymbol{j} \rangle$.

Let us now discover the connection between S and the reverberation time, which is connected in turn to $\boldsymbol{\nabla}\cdot\boldsymbol{U}$ and to the angular momentum, related to $\boldsymbol{\nabla}\wedge\boldsymbol{U}$.

Starting from the decomposition (16), we know that there exist a scalar field $H(\boldsymbol{x})$ and a vector field $\boldsymbol{G}(\boldsymbol{x})$, such that the two parts of the energy velocity field can be represented as

$$\boldsymbol{U}_{\mathrm{irr}}(\boldsymbol{x}) = \boldsymbol{\nabla}H(\boldsymbol{x}), \quad \boldsymbol{U}_{\mathrm{sol}}(\boldsymbol{x}) = \boldsymbol{\nabla}\wedge\boldsymbol{G}(\boldsymbol{x}). \tag{20}$$

The *energy-velocity potentials* H and $\boldsymbol{G}$ are not uniquely defined by these conditions: the addition to H of any constant (with respect to $\boldsymbol{x}$), or any irrotational vector to $\boldsymbol{G}$ do not change Eq. (20). The vector field $\boldsymbol{G}$, on its turn, can also undergo a decomposition of type (16), therefore, the generality of the treatment is not reduced by imposing on $\boldsymbol{G}$ the condition $\boldsymbol{\nabla}\cdot\boldsymbol{G} = 0$. If $K(\boldsymbol{x})$ and $\boldsymbol{R}(\boldsymbol{x})$ are a given scalar and a given vector field, substituting conditions (20) into the equations

$$\boldsymbol{\nabla}\cdot\boldsymbol{U} = K(\boldsymbol{x}), \quad \boldsymbol{\nabla}\wedge\boldsymbol{U} = \boldsymbol{R}(\boldsymbol{x})$$

and taking into account the identity $\boldsymbol{\nabla}\wedge(\boldsymbol{\nabla}\wedge\boldsymbol{G}) \equiv \boldsymbol{\nabla}(\boldsymbol{\nabla}\cdot\boldsymbol{G}) - \Delta\boldsymbol{G}$, we find that the potentials must satisfy Poisson's equations:

$$\Delta H(\boldsymbol{x}) = K(\boldsymbol{x}),$$

$$-\Delta\boldsymbol{G}(\boldsymbol{x}) = \boldsymbol{R}(\boldsymbol{x}).$$

The energy velocity field $\boldsymbol{U}(\boldsymbol{x})$ is determined by solving these equations with the proper boundary conditions. In the case of the unbounded space, the boundary conditions are replaced by asymptotic conditions, which are $H(\boldsymbol{x}), \boldsymbol{G}(\boldsymbol{x}) \to 0, (|\boldsymbol{x}| \to \infty)$, supposing that K and $\boldsymbol{R}$ decrease at infinity fast enough. The corresponding Green's function is

$$G_\infty(\boldsymbol{x},\boldsymbol{y}) = \frac{1}{4\pi|\boldsymbol{x}-\boldsymbol{y}|},$$

and the solutions:

$$H(\boldsymbol{x}) = \int_{\mathbb{R}^3} \frac{K(\boldsymbol{y})\mathrm{d}^3\boldsymbol{y}}{4\pi|\boldsymbol{x}-\boldsymbol{y}|}, \quad \boldsymbol{G}(\boldsymbol{x}) = -\int_{\mathbb{R}^3} \frac{\boldsymbol{R}(\boldsymbol{y})\mathrm{d}^3\boldsymbol{y}}{4\pi|\boldsymbol{x}-\boldsymbol{y}|}.$$

By calculating the gradient of H and the curl of $\boldsymbol{G}$, we find the final result

$$\boldsymbol{U}(\boldsymbol{x}) = \int_{\mathbb{R}^3} \frac{[K(\boldsymbol{y}) - \boldsymbol{R}(\boldsymbol{y})\wedge](\boldsymbol{x}-\boldsymbol{y})\,\mathrm{d}^3\boldsymbol{y}}{4\pi|\boldsymbol{x}-\boldsymbol{y}|^3}, \quad \boldsymbol{x} \in \mathbb{R}^3,$$

expressing the velocity $\boldsymbol{U}$ in terms of its divergence K and its curl $\boldsymbol{R}$.

Now, the divergence K is just the reciprocal of the time constant $\tau_0(\boldsymbol{x}) = [\boldsymbol{\nabla}\cdot\boldsymbol{U}(\boldsymbol{x},0)]^{-1}$, characterizing the energy evolution in steady states, which is related to the local rate constant of the exponential initial decay by $k = |1/\tau_0|$ giving the k-reverberation time as

$$T_{k60} = \frac{6\ln(10)}{k},$$

while (see Eq. (14)) the curl $\boldsymbol{R}$ can be expressed in terms of intensity $\boldsymbol{J}$ and energy density W as

$$\boldsymbol{R}(\boldsymbol{x}) = \boldsymbol{\nabla}\wedge\frac{\boldsymbol{J}(\boldsymbol{x})}{W(\boldsymbol{x})} = \frac{\boldsymbol{\nabla}\wedge\boldsymbol{J}(\boldsymbol{x}) + \boldsymbol{J}(\boldsymbol{x})\wedge\boldsymbol{\nabla}\ln W(\boldsymbol{x})}{W(\boldsymbol{x})}.$$

Taking into account Eq. (15), the average energy velocity $\boldsymbol{U}$ can thus be expressed as

$$\boldsymbol{U}(\boldsymbol{x}) = \int_{\mathbb{R}^3} \left[\frac{1}{\tau_0(\boldsymbol{y})} + 2[\boldsymbol{\Omega}_1(\boldsymbol{y}) + \boldsymbol{\Omega}_2(\boldsymbol{y})]\wedge\right] \frac{\boldsymbol{x}-\boldsymbol{y}}{4\pi|\boldsymbol{x}-\boldsymbol{y}|^3}\,\mathrm{d}^3\boldsymbol{y},$$

so clarifying that, when in a steady state, the sound radiation flows along $\boldsymbol{U}-$trajectories characterized by a wave conductance:

$$S(\boldsymbol{x}) = \rho_0 \left| \int_{\mathbb{R}^3} \left[\frac{1}{\tau_0(\boldsymbol{y})} + 2[\boldsymbol{\Omega}_1(\boldsymbol{y}) + \boldsymbol{\Omega}_2(\boldsymbol{y})]\wedge\right] \frac{\boldsymbol{x}-\boldsymbol{y}}{4\pi|\boldsymbol{x}-\boldsymbol{y}|^3}\,\mathrm{d}^3\boldsymbol{y} \right|.$$

We can conclude that the conduction of sound radiation by any sound field, not only depends on k-reverberation time through τ_0, but also on angular momentum, through $\boldsymbol{\Omega}_1$, and on the non-homogeneous distribution of energy in the field, through $\boldsymbol{\Omega}_2$.

A similar result, here derived for a free sound field, can be easily extended to the case of a bounded enclosure V. In this case, in the relevant expressions, one has only to replace the Green's function G_∞ by the Green's function of the Laplace

operator Δ with suitable boundary conditions on the surface enclosing V, $G_V(\boldsymbol{x},\boldsymbol{y})$:

$$\boldsymbol{U}(\boldsymbol{x}) = \int_V \left[\frac{1}{\tau_0(\boldsymbol{y})} + 2[\boldsymbol{\Omega}_1(\boldsymbol{y}) + \boldsymbol{\Omega}_2(\boldsymbol{y})]\wedge\right] \boldsymbol{\nabla}_{\boldsymbol{x}} G_V(\boldsymbol{x},\boldsymbol{y})\, \mathrm{d}^3\boldsymbol{y}, \quad \boldsymbol{x}\in V.$$

One then arrives to the grand conclusion that sound radiated from any steady source in any environment, is conducted by the wave field according to boundary conditions along trajectories with average velocity $\boldsymbol{U}$, which is completely determined by reverberation and rotation of energy, the latter being related to both angular momentum and to non-uniform energy distribution.

7. Conclusions

The main results of the present paper can be summarized in the following points:

(1) Any acoustical steady state in an enclosure begins its decay at any point $\boldsymbol{x}_0$, being driven by an exponential function of time with rate constant $k = |\boldsymbol{\nabla}\cdot\boldsymbol{U}(\boldsymbol{x}_0,0)|$, where $\boldsymbol{U}$ is the mean energy velocity.
(2) The statement (1) has been confirmed experimentally both for 1-D and 3-D environments. Specifically in a tube of dimensions $0.28\times 0.28\times 4\,\mathrm{m}^3$ with varying absorption properties and in a small room with a $104\,\mathrm{m}^3$ volume. Other experiments, showed similar results (see Ref. [18]).
(3) We have found an expression for the distribution of the energy velocity field $\boldsymbol{U}(\boldsymbol{x})$, showing how it depends not only on the time constant τ_0, but also on the distribution of angular momentum and on the non-uniformity of the energy density.

In conclusion, it can be said that the energy velocity field is one of the most pervasive concepts in acoustics and a powerful tool for modeling the energetics of any sound field. Moreover, it can be determined experimentally by means of the modern hyper-intensimetric techniques based on pressure–velocity probes, so allowing, in particular, the precise definition and measurement of reverberation time on a firm physical basis.

References

[1] R.V. Waterhouse, T.W. Yates, D. Feit, Y.N. Liu, Energy streamlines of a sound source, *J. Acoust. Soc. Am.* 78 (2) (1985) 758–762.
[2] R.V. Waterhouse, D.G. Crighton, J.E. Ffwocs-Williams, A criterion for an energy vortex in a sound field, *J. Acoust. Soc. Am.* 81 (1987) 1323.
[3] R.V. Waterhouse, Vortex modes in rooms, *J. Acoust. Soc. Am.* 82 (5) (1987) 1782–1791.
[4] G. Schiffrer, D. Stanzial, Energetic properties of acoustic fields, *J. Acoust. Soc. Am.* 96 (1994) 3645–3653.
[5] D. Stanzial, N. Prodi, G. Schiffrer, Reactive acoustic intensity for general fields and energy polarization, *J. Acoust. Soc. Am.* 99 (1996) 1868–1876.
[6] D. Stanzial, Sound energy transfer velocity, a fundamental concept in architectural acoustics, *Proceedings of W. A. Sabine Centennial Symposium*, MIT, Cambridge, MA, USA, 5–7 June 1994, pp. 251–254.
[7] J. Zhe, Intensity streamlines and vorticity streamlines in three dimensional sound fields, *J. Acoust. Soc. Am.* 107 (2) (2000) 725–730.
[8] M.R. Schroeder, New method of measuring reverberation time, *J. Acoust. Soc. Am.* 37 (1965) 409–412.
[9] M.R. Schroeder, Circularly polarized acoustic fields: the number theory connection, *Acustica* 75 (1991) 94–98.
[10] D. Stanzial, D. Bonsi, G. Schiffrer, Four-dimensional treatment of linear acoustic fields and radiation pressure, *Acta Acustica—Acustica* 89 (2003) 213–224.
[11] L. Landau, E. Lifchitz, *Physique theorique, Mécanique des fluides*, Tome 6, 2^e édition, MIR, Moscou, 1989, pp. 19–20.
[12] W.C. Sabine, *Collected Papers on Acoustics Chapter 1 "Reverberation"*, third Impression, Harvard University Press, Cambridge, MA, USA, 1927, pp. 3–68.
[13] W.B. Joyce, Sabine's reverberation time and ergodic auditoriums, *J. Acoust. Soc. Am.* 58 (3) (1975) 643–655.
[14] K.H. Kuttruff, Sound decay in enclosures with non-diffuse sound field, *Proceedings of W. A. Sabine Centennial Symposium*, Cambridge, MIT, MA, USA, 5–7 June 1994, pp. 85–88.
[15] G. Sacchi, D. Stanzial, A new method for axial $p-v$ probe calibration, *Proceedings of XVI International Congress of Sound and Vibration (ICSV)*, Kraców, 5–7 July 2009, Session S35, paper 765.
[16] F. Jacobsen, V. Jaud, A note on the calibration of pressure velocity sound intensity probes, *J. Acoust. Soc. Am.* 120 (2) (2006) 830–837.
[17] J. Wolfe, J. Smith, J. Tann, N. H Fletcher, Acoustic impedance of classical and modern flutes, *J. Sound Vib.* 243 (2001) 127–144.
[18] D. Stanzial, Sabine's formula revisited with acoustic quadraphony, *Proceedings of the 19th International Congress on Acoustics*, Madrid 2–7 September 2007. Revised Edition—⟨http://www.sea-acustica.es/WEB_ICA_07/fchrs/papers/rba-16-003.pdf⟩.